Journal of Power Technologies 102 (3) (2022) 108 -- 120

Energy analysis and optimizing of hybrid WT/ PV cell in power systems

Reza Alayi*[1], Mehrdad Ahmadi Kamarposhti [2], Mohsen Ghafari[3], Salamoulah Mohammadi Aylar[1]

[1]Departement of mechanics, Germi Branch, Islamic Azad University, Germi, Iran.

reza.alayi@yahoo.com – reza_alayi@iaugermi.ac.ir

[2] Department of Electrical Engineering, Jouybar Branch, Islamic Azad University, Jouybar, Iran

[3] Department of Electrical Engineering, Daneshestan Institute of Higher Education, Saveh, Iran.

Abstract

The importance placed on renewable energy is growing exponentially due to rising demand for energy, concerns about the environmental impact of burning fossil fuels and fears about the world's limited fossil fuel reserves. This study features an optimal combination of scattered production sources (wind-solar), an IEEE 33-bus system, and beta distribution to model wind speed. The load and production planning period is 24 hours. The aim of this study is to improve voltage profiles, increase reliability and reduce losses. The resulting model forecast a 39% loss-improvement in the presence of wind turbines and a 40% loss-improvement in the presence of photovoltaic cells, which highlights the role of these renewable resources in the grid.

Introduction

Since distribution networks are well-suited for connecting to the power system, the most important step in using Distributed Generation (DG) is to place DG systems in distribution networks and achieve optimal capacity. This is important because it reduces costs associated with casualties, reliability, and the cost of building production units [1–3] and pylons. On the other hand, uncertainty is one of the most important factors increasing risk in the planning of power systems, so failure to consider this parameter can lead to significant economic and technical losses.

Distributed generation sources are now widely used in electrical systems due to their importance in energy production[4,5]. Sincron generators are one of the most common forms of dispersed products installed in medium pressure distribution systems. Because of the type of synchronous generator, DG performance capabilities, which have different operating modes such as power factor and voltage control, as well as the ability to operate in different locations, can also affect the performance of voltage control and reactive power equipment[6–8]. Therefore, to ensure that ULTC and especially DG do not adjust the appropriate voltage in the system, distribution system units must be connected to the grid in coordination with other equipment of the system [9,10].

Several studies have been proposed on the control of voltage and reactive power in electrical energy distribution systems without examining the effect of DG [11–15]. Given the scope of the problem, most research has sought to achieve the best response in the shortest possible time, with only feeder capacitors being subject to optimal voltage and reactive power control, while low capacitors are not considered [16–18].

In order to solve the multi-objective problem of voltage control and reactive power, the phase building of target and constraint functions as well as the metal hardening algorithm have been used to determine the final answer [19,20]. To reduce the search space, a time-based algorithm was used to predict the 24-hour forecast in order to determine the position of the pulse at any time interval, as well as the genetic algorithm to determine the optimal response [21]. Voltage and reactive power control was conducted in the presence of a scattering source of induction machine (wind turbine) and using a combination of local and centralized control of equipment [21,22]. Feeder capacitors are controlled by a local voltage type controller: an abnormal position in the controller. The changer's low and high capacitors can be remotely controlled on a daily basis. In both local and proposed controls, DG and the effect of how the change control function has been proposed were investigated. Reactive voltage and power control is performed in the presence of scattered generator-based generator sources, and it is assumed that all equipment has only local control capability.

Meanwhile, assuming that the distribution system is automated, centralized control of control equipment is conducted at any time of the day and night, observing the prevailing restrictions and with objectives such as: reducing losses and improving voltage profiles. This control is done in two modes with and without the presence of a scattered production source and in two modes of power: factor control and voltage control. Also in the considered problem, DG is the effect of location and capacity. Due to the discrete space of the optimization problem, the genetic algorithm was used to optimize and determine the position of the equipment 24 hours a day. Driving a series of developments in transmission and distribution technology have been the design and operation of power systems with maximum efficiency, maximum reliability and safety. This is also the case with reactive power control in transmission and distribution networks. The desired goals are in particular to increase the transmission capacity of existing lines, prevent rapid and large changes in the voltage level, improve the power factor, and balance the load.

Materials and methods

Network Modeling 33-Bus Considering Load Uncertainty and Production

This section reports on the modeling of the 33-bus network in a 24-hour, seasonal manner with uncertainty of load and production. The modeling is tested against a reference. We modeled the 33-bus network with a new arrangement and compared the results for the voltage, loss, and network security profiles with a previous 33-bus distribution network layout, to see the effect of the new layout on the network's basic parameters and in real time. Full information will be provided regarding the IEEE 33-bus standard standard network. The network is shown schematically in 1.

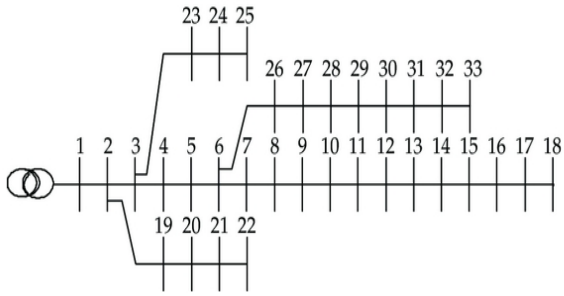

Figure 1. Schematic diagram of IEEE 33-bus bar network

As you can see from 1 the 33-bus network consists of four main branches that are connected to the transmission network via a 1-bus and a transformer. Information about this network, including the maximum active and reactive power of the network, the resistance value and the reactance of the lines, is given in 1 and 2.

Solar and wind

2 shows the hourly generation using wind and solar sources. The figure on the right shows wind and on the left sun. In addition to being hourly, the production rate is also shown seasonally. Weibull distribution is used for wind and beta distribution for solar.

Electrical load

The following figure shows power consumption per hour for different seasons. To show the uncertainty of the load, load planning was considered as 24-hour and seasonal. That way, we can bring the simulation results closer to reality, with the possibility of load and production.

Table 1: Maximum amount of active and reactive power of 33-bus network

Bus number	**2**	**3**	**4**	**5**	**6**	**7**	**8**	**9**
P_L(kW)	100	90	120	60	60	200	200	60
q_L(Kvar)	60	40	80	30	20	10	10	20
Bus number	**10**	**11**	**12**	**13**	**14**	**15**	**16**	**17**
P_L(kW)	60	45	60	60	120	60	60	60
q_L(Kvar)	20	30	35	35	80	10	20	20
Bus number	**18**	**19**	**20**	**21**	**22**	**23**	**24**	**25**
P_L(kW)	90	90	90	90	90	90	420	420
q_L(Kvar)	40	40	40	40	40	50	200	200
Bus number	**26**	**27**	**28**	**29**	**30**	**31**	**32**	**33**
P_L(kW)	60	60	60	120	200	1505	210	60
q_L(Kvar)	25	25	20	10	60	70	10	40

Table 2. Resistance and reactance values of 33-bus network lines

Line number	**1-2**	**2-3**	**3-4**	**4-5**	**5-6**	**6-7**	**7-8**	**8-9**
n_k	0.0922	0.4930	0.3660	0.3811	0.8190	0.1872	0.7114	1.0300
X_k	0.0470	0.2511	0.1846	0.1941	0.7070	0.6188	0.2351	0.7400
Bus number	**9-10**	**10-11**	**11-12**	**12-13**	**13--14**	**14-15**	**15-16**	**16-17**
n_k	1.04	0.19	0.37	1.46	0.54	0.59	0.74	1.28
X_k	0.74	0.06	0.12	1.15	0.71	0.52	0.54	1.72
Bus number	**17-18**	**18-19**	**19-20**	**20-21**	**21-22**	**22-23**	**23-24**	**24-25**
n_k	0.73	0.16	1.50	0.40	0.70	0.45	0.89	0.89
X_k	0.57	0.15	1.35	0.47	0.93	0.30	0.70	0.70
Bus number	**6-27**	**26-27**	**27-28**	**28-29**	**29-30**	**30-31**	**31-32**	**32-33**
n_k	0.20	0.28	1.05	0.80	0.50	0.97	0.31	0.34
X_k	0.10	0.14	0.93	0.70	0.25	0.96	0.36	0.53

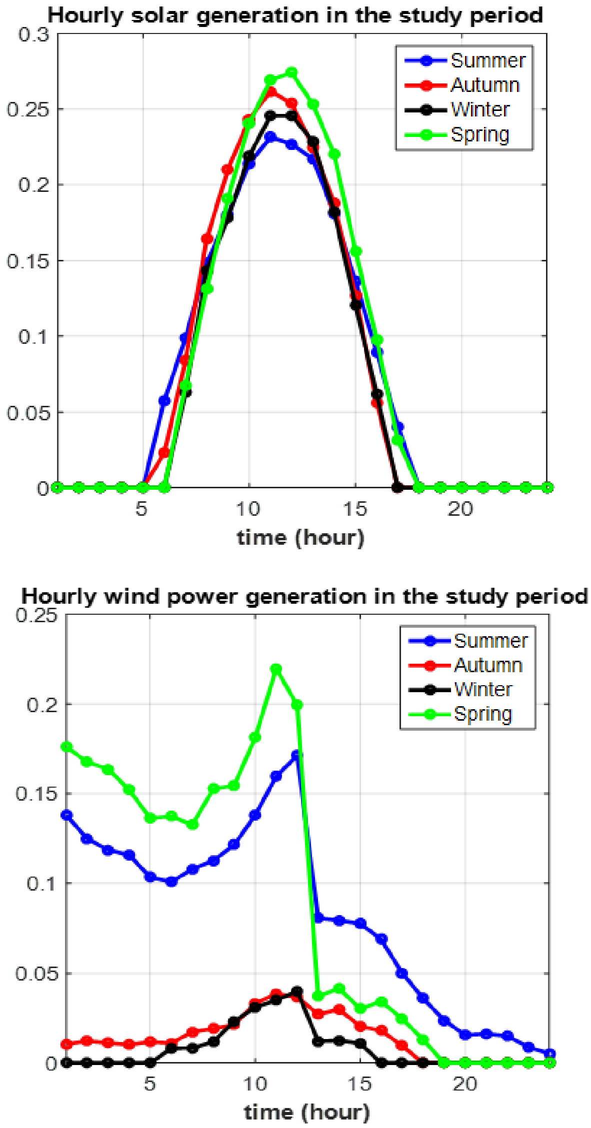

Figure 2. Wind and solar production per hour

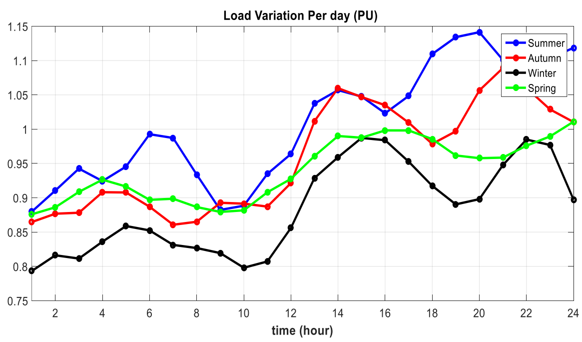

Figure 3. Power consumption per hour

Possible power generation model

Wind and solar generation is affected by weather conditions such as sunlight, wind speed and ambient temperature. Probability distribution functions (PDFs) can be used in a statistical manner to identify the random behavior of a renewable source (wind speed and solar radiation). The probability of solar radiation was considered following the Beta PDF. The beta distribution of solar radiation (kw/m^2) s^t during the time segment t́ is as follows[20].

$$f_s^t(s) = \frac{\Gamma(\alpha^t + \beta^t)}{\Gamma(\alpha^t)\,.\,\Gamma(\beta^t)} \cdot (s^t)^{\alpha^t - 1}.(1 - s^t)^{\beta^t - 1} \; for \;\; \alpha^t > 0; \;\; \beta^t > 0 \tag{1}$$

Here $\beta^{t\&}$ α^t are parameter forms in t, and Γ also indicates the gamma function. The shape of the Beta PDF parameters can be calculated using the mean (μ_s^t) and standard deviation $(\sigma_s^t)$of radiation for the relevant time segment.

$$\beta^t = (1 - \mu_s^t)\,.\left(\frac{\mu_s^t(1 + \mu_s^t)}{(\sigma_s^t)^2} - 1\right) \tag{2}$$

$$\alpha^t = \frac{\mu_s^t * \beta^t}{(1 - \mu_s^t)} \tag{3}$$

The decision to describe the random behavior of wind speeds is selected in a predetermined period of time Weibull PDF. The distribution of Weibull for wind speed V^t (m/s) in the time interval tm can be expressed as follows [23,24]

$$f_v^t(v) = \frac{k^t}{c^t} \cdot \left(\frac{v^t}{c^t}\right)^{k^t - 1} .\exp\left(-\left(\frac{v^t}{c^t}\right)^{k^t - 1}\right) \;\; for \;\; c^t > 1: \;\; k^t > 0 \tag{4}$$

The parameter (k^t) and the scale factor (c^t) in the time segment tm are calculated as follows:

$$k^t = \left(\frac{\sigma^t}{\mu_v^t}\right)^{-1.086} \tag{5}$$

$$c^t = \frac{\mu_v^t}{\Gamma\left(1 + {}^{1}/_{k^t}\right)} \tag{6}$$

μ_V^t And σ_V^t are the mean standard wind deflection deviations in time segment t. To calculate the output power of wind and solar DGs, continuous PDFs are divided into periods for a specific time frame. In each of them, solar radiation and wind speed are at a certain level. Production of Pv and WT array power is controlled by the probability of all possible states for that time.

The average hourly output power of a PV array is related to a specific time segment $t\left(P_{pv}^t\right)$which can be calculated as follows: [23].

$$P_{PV}^t = \sum_{g=1}^{N_s} PG_{PVg} * P_s\left(s_g^t\right) \tag{7}$$

Here g determines the variable of state (period) and Ns the number of discrete states of solar radiation. S_g^t Is also g a_{min} state / solar radiation level in t a_{min} time fragment. The probability of solar radiation for each state for each specific time frame is calculated as follows:[24]

$$P_s\left(s_g^t\right) = \begin{cases} \int_0^{(s_g^t+s_{g+1}^t)/2} f_s^t(s)ds & \text{for } g = 1 \\ \int_{(s_{g-1}^t+s_g^t)/2}^{(s_g^t+s_{g+1}^t)/2} f_s^t(s)ds & \text{for } g = 2 \ldots (N_s - 1) \\ \int_{(v_{S-1}^t+v_S^t)/2}^{\infty} f_s^t(s)ds & \text{for } g = N_s \end{cases} \tag{8}$$

Sunlight and ambient temperature are the main factors influencing the output power of the Pv array. The power output of the Pv array in average solar radiation (sag) for g $_{amin}$ state / level is evaluated as follows. [23]

$$PG_{PVg}\left(s_{ag}\right) = N_{PVmod} * FF * V_g * I_g \tag{9}$$

Here Npvmod is the sum of the number of Pv modules used for a Pv array. The current-voltage characteristic of the Pv module can be determined for a specific radiation level and ambient temperature T_A (°C) using the following equations [23,24]

$$I_g = s_{ag}[I_{SC} + K_i(T_C - 25)] \tag{10}$$

$$V_g = V_{OC} - K_v * T_{cg} \tag{11}$$

$$T_{cg} = T_A + s_{ag}\left(\frac{N_{OT} - 20}{0.8}\right) \tag{12}$$

$$FF = \frac{V_{MPP} * I_{MPP}}{V_{OC} * I_{SC}} \tag{13}$$

T_cg temperature of the solute in g Amin is the state of k_v and k_I; (°C) is the coefficient of current and voltage temperature (A⁄ °C and V⁄ °C); N_OT is the nominal operating temperature of the cell; FFt (°C) is the filling factor; V_OC and I_SC are open circuit voltage (V) and the short circuit current (A) L_MPP and V_MPP are also the voltage (V) and current (A) at the maximum power point, respectively.

$$P_{WT}^t = \sum_{g=1}^{N_v} PG_{WTg} * P_v\left(v_g^t\right) \tag{14}$$

The probability of wind speed for each mode during each specific time frame is calculated as follows:[20]

$$P_v\left(v_g^t\right) = \begin{cases} \int_0^{(v_g^t+v_{g+1}^t)/2} f_v^t(v)dv & \text{for } g = 1 \\ \int_{(v_{g-1}^t+v_g^t)/2}^{(v_g^t+v_{g+1}^t)/2} f_v^t(v)dv & \text{for } g = 2 \ldots (N_v - 1) \\ \int_{(v_{g-1}^t+v_g^t)/2}^{\infty} f_v^t(v)dv & \text{for } g = N_v \end{cases} \tag{15}$$

WT power generation depends on its power performance curve. For nonlinear performance characteristics, the production of WT power at average wind speed (V_ag) for mode (g) is calculated as follows.

$$PG_{WTg} = \begin{cases} 0 & v_{ag} < v_{cin} \text{ or } v_{ag} > v_{cout} \\ \left(a * v_{ag}^3 + b * P_{rated}\right) & v_{cin} \le v_{ag} \le v_N \\ P_{rated} & v_N \le v_{ag} \le v_{cout} \end{cases} \tag{16}$$

Here P_{rated} is the maximum power that can be generated through WT. V_{cout} The wind speed is maximum. Fixes a and b are a function of the minimum wind speed V_{cin} and the nominal wind speed (V_N), which are calculated as follows:

$$a = \frac{P_{rated}}{(v_N^3 - v_{cin}^3)} \tag{17}$$

$$b = \frac{v_{cin}^3}{(v_N^3 - v_{cin}^3)} \quad (18)$$

Since DG distribution networks are active networks, performance and control of the network are key issues. Although there are a number of issues with the distribution network's performance, there are also major technical implications due to the influence of renewable DGs, such as network power loss, voltage stability, and network security discussed here.

Distribution networks are usually radially structured to reduce the complexity of protection. Assessing and reducing network power losses is essential to increase system efficiency. The average power loss per year can be calculated as follows:

$$Ploss_a = \frac{\sum_{t=1}^{N_t} \sum_{i=1}^{N_b} \frac{r_i((P_{D.i+1}^t)^2 + (Q_{D.i+1}^t)^2)}{(V_{i+1}^t)^2}}{N_t} \quad (19)$$

Here Q_(D.i+1)^t and P_(D.i+1)^t are the demand for active and reactive power in the receiver end bus -i + 1 for t amen. V_(i+1)^t The amplitude of the voltage at the end bus receiving the -i + 1 for t is the time interval. ri The resistance of the completed transmission line to bus Nl, -i + 1 is the sum of the number of lines in the system and Nt is the sum of the number of time pieces considered in a year.

Voltage stability indicators are used to assess the level of voltage stability of buses in the transmission or distribution network. These are very fast and effective tools for calculating the offline stability of voltage buses. The voltage stability index VSF (Voltage Stability Factor) for each bus -i + 1 in time interval t can be expressed as follows.

$$VSF_{i+1}^t = (2V_{i+1}^t - V_i^t) \quad (20)$$

The average annual voltage stability for the entire distribution network can be calculated as follows:

$$VSF_a = \frac{\sum_{t=1}^{N_t} \sum_{i=2}^{N_b} VSF_{i+1}^t}{N_t(N_b - 1)} \quad (21)$$

N_b is the sum of the number of buses in the network. The bus -i + 1 is assumed to be in the main distribution post. The researchers looked at how high the VSF was. The network is more stable. If the line capacity increases from the existing transmission capacity, it will be overloaded, which is likely to cause network congestion, which in turn will cause various types of network disruptions. Line load (LL) is the load distribution (MVA) on the line according to the maximum power capacity (MVA), which is expressed for line i during time interval "t" as follows:

$$LL_i^t = \frac{L_{MVA.i}^t}{L_{MVA_{max}.i}} \quad (22)$$

Here $L_{MVA_{max.i}}^t$ and $L_{MVA.i}^t$ is the real capacity and maximum line i in t is the time interval. The annual average network security index (NSI) is plotted according to the loading of all lines in the network, which is as follows:

$$NSI_a = \frac{\sum_{t=1}^{N_t} \sum_{i=1}^{N_l} LL_i^t}{N_t * N_l} \quad (23)$$

Lower NSI values indicate a lower power risk than lines, which in turn increases network security. The proposed planning method should provide the equality and inequality constraints described below.

$$PG = \sum_{i=2}^{Nb} Pd.i \; - Ploss = 0 \quad (24)$$

$$QG_{ss} - \sum_{i=2}^{Nb} Qd.i \; - Qloss = 0 \quad (25)$$

PG_{ss}^t and QG_{ss}^tThe active and reactive power fed by mail in t is the timepiece. Lo Qloss. $Qloss^t$ And $Ploss^t$T are the loss of active and reactive power in t is the time frame.

$$V_i^t \leq V_{max.i} \quad (26)$$

$V_i^t$and $V_{max.i}$are the actual and maximum voltages in bus i for time interval t.

$$L_{MVA.i}^t \leq L_{MVA_{max.i}} \quad (27)$$

$L_{MVAmax}^t$and L_{MVAi}^tt are the maximum and actual loads of line i in time interval t.

Photovoltaic cell and wind turbine

The renewable energy sources used in this system are PV cells and wind turbines. The specifications of the wind turbine and PV cell can be seen in 3 and 4.

Table 3. PV module specifications

Parameter	Unit	Amount
Voltage at the maximum point of VMPP power	V	28.36
Flow at the maximum IMPP power point	A	7.76
Open circuit voltage Voc	V	36.96
Short circuit current	A	8.38
Nominal operating cell temperature NOT	℃	43
Thermal flow	A/℃	0.00545
Thermal voltage	V/℃	0.1278

Table 4. Wind turbine specifications

Parameter	Unit	Amount
Permitted nominal output power Prated	kW	250
Internal cutting speed V_{cin}	m/s	3
Nominal wind speed V_N	m/s	12
External cutting speed V_{cout}	m/s	25

As can be seen from Table 3, the maximum power output for the PV cell is 220 W. As can be seen from Table 4, the maximum power output of the wind turbine is 250 kW, this production capacity is possible for wind speeds of 12 m/s or more, the cutting speed for the turbine is 25 m/s.

Results

Results with scattered production sources

Figure 4 shows the amount of electricity generated by the wind turbine and PV cell regardless of the grid. Figure 5 shows the amount of electricity generated by the wind turbine and the PV cell, taking into account the grid mentioned in the previous section.

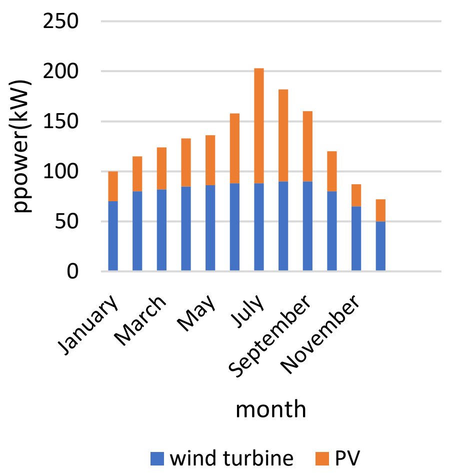

Figure 4. Wind turbine and PV generation without grid

As can be seen in Figure 4, the PV cell outperforms the wind turbine only in July. The wind turbine's highest and lowest electrical production figures are in August and December respectively. For August electrical production is 90 kW/day and for December 50 kW/day. The PV cell's highest and lowest electrical production figures are in July and December: 118 and 22 kW/day, respectively.

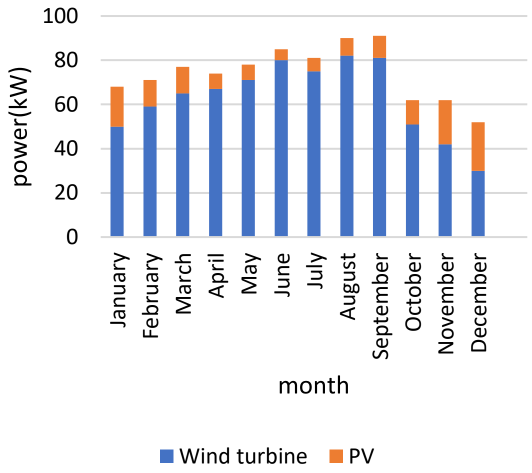

Figure 5. Wind turbine and PV generation with grid

As shown in Figure 5, the highest and lowest electrical production of the renewable energy system are in September and December. For September electrical production is 91 kW/day and for December 50 kW/day. In September, the wind turbine produces 81 kW/day and the PV cell 10 kW/day. In December, the wind turbine produces 30 kW/day and the PV cell 22 kW/day.

The problem is solved as a multi-objective task, and the results show that the system parameters have been improved in multi-objective mode. The following tables show the parameters used for simulation. Figure 6 shows the value of the objective function in different iterations and how to achieve the optimal answer in different iterations. As can be seen, the algorithm reached the optimal answer after 8 repetitions.

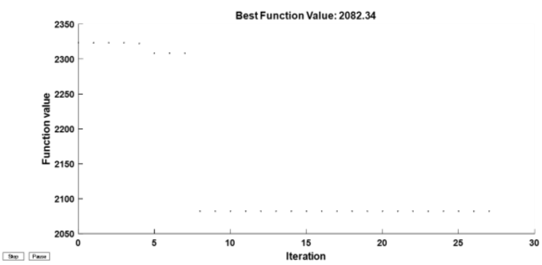

Figure 6. The optimal answer of the algorithm for different iterations

Table 5 shows the simulation results in the first scenario as a single goal and in the second scenario as a multi-objective. As can be seen, voltage stability in both scenarios is almost equal, but the system security index and multi-objective loss improvements have improved compared to single-target mode.

Table 5. Simulation results for 33-bus system with uncertainty

	Security Index	Voltage Profile	Losses	Location of scattered products
Primary system	0.59	0.91	0.89	—
WT	0.386	0.9288	0.3929	2 5 4 4
PV	0.3772	0.9228	0.4065	5 4 4 4
Optimal (Scenario 1)	0.386	0.9288	0.3922	27 17 13 11
Optimal (Scenario 2)	0.3331	0.919	0.3388	17 9 8 7

Figure 7 shows the multi-objective optical beam curve. As can be seen, the front beam provides a set of answers for the objective functions.

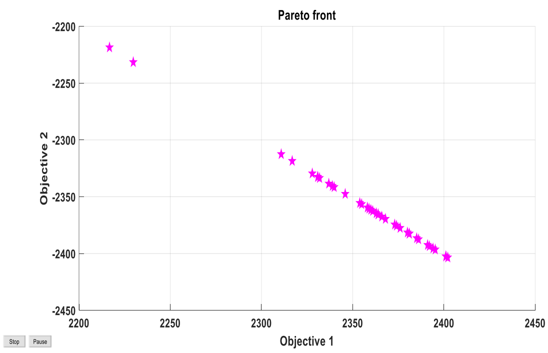

Figure 7. Front beam curve related to multi – objective optimization

Figure 8 shows the amount of electrical power generated by the wind turbine and the PV cell, taking into account the limitations, including optimization.

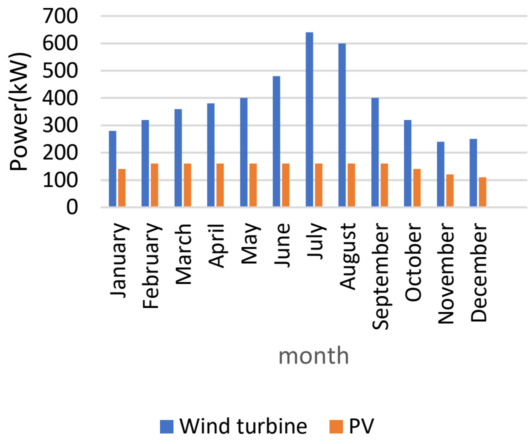

Figure 8. Optimal Wind turbine and PV generation with grid

In Figure 8, the wind turbine's highest power generation is in July, with 640 kW/day. PV production in July is 160 kW/day. The wind turbine's lowest power generation is in November, with 240 kW/day. PV production in November is 120 kW/day. The highest and lowest power generation months for wind turbines and PV cells combined are July and November. The total electricity produced for July and November is 800 and 360 kW/day, respectively.

Conclusion

Renewable energy sources have attracted a great deal of attention due to their virtually emissions-free operation. Recently, a significant number of distributed generation products (DGs) with intermittent production patterns have connected to the distribution network. Integrating renewable DGs into distribution networks is essential to ensure security of supply and good quality of electricity in the network. This paper presents a simple and effective method for sizing and optimizing the placement of wind and solar DGs in distribution locations, with a view to minimizing the loss of network power, and improving voltage stability and network security. Sunlight and wind speeds were also considered using appropriate models. Weighted particle optimization with weight accumulation was also used to optimize target functions in which the bus voltage limit, line loading capacity, discrete size limit and DG penetration limits are considered.

References

[1] Jain S, Kalambe S, Agnihotri G, Mishra A. Distributed generation deployment: State-of-the-art of distribution system planning in sustainable era. Renewable and Sustainable Energy Reviews 2017;77:363–85. https://doi.org/10.1016/J.RSER.2017.04.024.

[2] Eltamaly AM, Sayed Mohamed Y, El-Sayed A-HM, Nasr A, Elghaffar A. Reliability / Security of Distribution System Network under Supporting by Distributed Generation. Insight - Energy Science 2019;2:1–14. https://doi.org/10.18282/i-es.v2i1.181.

[3] Alayi R, Kasaeian A, Atabi F. Thermal analysis of parabolic trough concentration photovoltaic/thermal system for using in buildings. Environmental Progress & Sustainable Energy 2019;38:13220. https://doi.org/10.1002/EP.13220.

[4] Tribioli L, Cozzolino R. Techno-economic analysis of a stand-alone microgrid for a commercial building in eight different climate zones. Energy Conversion and Management 2019;179:58–71. https://doi.org/10.1016/J.ENCONMAN.2018.10.061.

[5] Alayi R, Jahanbin F. Generation Management Analysis of a Stand-alone Photovoltaic System with Battery. Renewable Energy Research and Applications 2020;1:205–9. https://doi.org/10.22044/RERA.2020.9492.1026.

[6] Cavalcanti D, Perez-Ramirez J, Rashid MM, Fang J, Galeev M, Stanton KB. Extending Accurate Time Distribution and Timeliness Capabilities over the Air to Enable Future Wireless Industrial Automation Systems. Proceedings of the IEEE 2019;107:1132–52. https://doi.org/10.1109/JPROC.2019.2903414.

[7] Nguyen HT, Battula S, Takkala RR, Wang Z, Tesfatsion L. An integrated transmission and distribution test system for evaluation of transactive energy designs. Applied Energy 2019;240:666–79.

https://doi.org/10.1016/J.APENERGY.2019.01.178.

[8] Esmaeili S, Anvari-Moghaddam A, Jadid S, Guerrero JM. Optimal simultaneous day-ahead scheduling and hourly reconfiguration of distribution systems considering responsive loads. International Journal of Electrical Power & Energy Systems 2019;104:537–48. https://doi.org/10.1016/J.IJEPES.2018.07.055.

[9] Valverde G, Shchetinin D, Hug-Glanzmann G. Coordination of distributed reactive power sources for voltage support of transmission networks. IEEE Transactions on Sustainable Energy 2019;10:1544–53. https://doi.org/10.1109/TSTE.2019.2892671.

[10] Murty VVVSN, Sharma AK. Optimal coordinate control of OLTC, DG, D-STATCOM, and reconfiguration in distribution system for voltage control and loss minimization. International Transactions on Electrical Energy Systems 2019;29:e2752. https://doi.org/10.1002/ETEP.2752.

[11] Kim I, Harley RG. Examination of the effect of the reactive power control of photovoltaic systems on electric power grids and the development of a voltage-regulation method that considers feeder impedance sensitivity. Electric Power Systems Research 2020;180:106130. https://doi.org/10.1016/J.EPSR.2019.106130.

[12] Ampofo DO, Myrzik JMA. A Comparative Study of Different Local Reactive Power Control Methods of Distributed Generation in Ghana. IEEE PES/IAS PowerAfrica Conference: Power Economics and Energy Innovation in Africa, PowerAfrica 2019 2019:504–9. https://doi.org/10.1109/POWERAFRICA.2019.8928779.

[13] Eltamaly AM, Mohamed YS, El-Sayed AHM, Elghaffar ANA. Analyzing of wind distributed generation configuration in active distribution network. 2019 8th International Conference on Modeling Simulation and Applied Optimization, ICMSAO 2019 2019. https://doi.org/10.1109/ICMSAO.2019.8880291.

[14] Liu W, Chen Y, Wang L, Liu N, Xu H, Liu Z. An Integrated Planning Approach for Distributed Generation Interconnection in Cyber Physical Active Distribution Systems. IEEE Transactions on Smart Grid 2020;11:541–54. https://doi.org/10.1109/TSG.2019.2925254.

[15] Mahdad B. Optimal reconfiguration and reactive power planning based fractal search algorithm: A case study of the Algerian distribution electrical system. Engineering Science and Technology, an International Journal 2019;22:78–101. https://doi.org/10.1016/J.JESTCH.2018.08.013.

[16] Muminovic Z, Dedovic MM, Avdakovic S. Optimal capacitor placement in low voltage distribution grid. ICAT 2019 - 27th International Conference on Information, Communication and Automation Technologies, Proceedings 2019. https://doi.org/10.1109/ICAT47117.2019.8938988.

[17] Hao Y, Yi Y, Tang J, Shi M. Active Reactive Power Control Strategy Based on Electrochemical Energy Storage Power Station. 2019 3rd IEEE Conference on Energy Internet and Energy System Integration: Ubiquitous Energy Network Connecting Everything, EI2 2019 2019:90–4. https://doi.org/10.1109/EI247390.2019.9062188.

[18] Chen J, Xu J, Zhong S. Optimal Voltage Control for Active Distribution Networks. ISPEC 2019 - 2019 IEEE Sustainable Power and Energy Conference: Grid Modernization for Energy Revolution, Proceedings 2019:382–91. https://doi.org/10.1109/ISPEC48194.2019.8974988.

[19] Huang Z, Fang B, Deng J. Multi-objective optimization strategy for distribution network considering V2G-enabled electric vehicles in building integrated energy system. Protection and Control of Modern Power Systems 2020;5. https://doi.org/10.1186/s41601-020-0154-0.

[20] Saffari M, Kia M, Vahidinasab V, Mehran K. Integrated active/reactive power scheduling of interdependent microgrid and EV fleets based on stochastic multi-objective normalised normal

constraint. IET Generation, Transmission & Distribution 2020;14:2055–64. https://doi.org/10.1049/IET-GTD.2019.1406.

[21] Alayi R, Kasaeian A, Atabi F. Optical modeling and optimization of parabolic trough concentration photovoltaic/thermal system. Environmental Progress & Sustainable Energy 2020;39:e13303. https://doi.org/10.1002/EP.13303.

[22] Marefati M, Shamel A, Alayi R, Gholaminia B, Rohi H. Designing a PID controller to control a fuel cell voltage using the imperialist competitive algorithm. Advances in Science and Technology Research Journal 2016;Vol. 10:176–81. https://doi.org/10.12913/22998624/62629.

[23] Zhang X, Liu J, Liu T, Zhou L. A novel power distribution strategy for parallel inverters in islanded mode microgrid. Conference Proceedings - IEEE Applied Power Electronics Conference and Exposition - APEC 2010:2116–20. https://doi.org/10.1109/APEC.2010.5433528.

[24] Lappalainen K, Valkealahti S. Output power variation of different PV array configurations during irradiance transitions caused by moving clouds. Applied Energy 2017;190:902–10. https://doi.org/10.1016/J.APENERGY.2017.01.013.

[1] Jain S, Kalambe S, Agnihotri G, Mishra A. Distributed generation deployment: State-of-the-art of distribution system planning in sustainable era. Renewable and Sustainable Energy Reviews 2017;77:363–85. https://doi.org/10.1016/J.RSER.2017.04.024.

[2] Eltamaly AM, Sayed Mohamed Y, El-Sayed A-HM, Nasr A, Elghaffar A. Reliability / Security of Distribution System Network under Supporting by Distributed Generation. Insight - Energy Science 2019;2:1–14. https://doi.org/10.18282/i-es.v2i1.181.

[3] Alayi R, Kasaeian A, Atabi F. Thermal analysis of parabolic trough concentration photovoltaic/thermal system for using in buildings. Environmental Progress & Sustainable Energy 2019;38:13220. https://doi.org/10.1002/EP.13220.

[4] Tribioli L, Cozzolino R. Techno-economic analysis of a stand-alone microgrid for a commercial building in eight different climate zones. Energy Conversion and Management 2019;179:58–71. https://doi.org/10.1016/J.ENCONMAN.2018.10.061.

[5] Alayi R, Jahanbin F. Generation Management Analysis of a Stand-alone Photovoltaic System with Battery. Renewable Energy Research and Applications 2020;1:205–9. https://doi.org/10.22044/RERA.2020.9492.1026.

[6] Cavalcanti D, Perez-Ramirez J, Rashid MM, Fang J, Galeev M, Stanton KB. Extending Accurate Time Distribution and Timeliness Capabilities over the Air to Enable Future Wireless Industrial Automation Systems. Proceedings of the IEEE 2019;107:1132–52. https://doi.org/10.1109/JPROC.2019.2903414.

[7] Nguyen HT, Battula S, Takkala RR, Wang Z, Tesfatsion L. An integrated transmission and distribution test system for evaluation of transactive energy designs. Applied Energy 2019;240:666–79. https://doi.org/10.1016/J.APENERGY.2019.01.178.

[8] Esmaeili S, Anvari-Moghaddam A, Jadid S, Guerrero JM. Optimal simultaneous day-ahead scheduling and hourly reconfiguration of distribution systems considering responsive loads. International Journal of Electrical Power & Energy Systems 2019;104:537–48. https://doi.org/10.1016/J.IJEPES.2018.07.055.

[9] Valverde G, Shchetinin D, Hug-Glanzmann G. Coordination of distributed reactive power sources for voltage support of transmission networks. IEEE Transactions on Sustainable Energy 2019;10:1544–53. https://doi.org/10.1109/TSTE.2019.2892671.

[10] Murty VVVSN, Sharma AK. Optimal coordinate control of OLTC, DG, D-STATCOM, and reconfiguration in distribution system for voltage control and loss minimization. International Transactions on Electrical Energy Systems 2019;29:e2752. https://doi.org/10.1002/ETEP.2752.

[11] Kim I, Harley RG. Examination of the effect of the reactive power control of photovoltaic systems on electric power grids and the development of a voltage-regulation method that considers feeder impedance sensitivity. Electric Power Systems Research 2020;180:106130. https://doi.org/10.1016/J.EPSR.2019.106130.

[12] Ampofo DO, Myrzik JMA. A Comparative Study of Different Local Reactive Power Control Methods of Distributed Generation in Ghana. IEEE PES/IAS PowerAfrica Conference: Power Economics and Energy Innovation in Africa, PowerAfrica 2019 2019:504–9. https://doi.org/10.1109/POWERAFRICA.2019.8928779.

[13] Eltamaly AM, Mohamed YS, El-Sayed AHM, Elghaffar ANA. Analyzing of wind distributed generation configuration in active distribution network. 2019 8th International Conference on Modeling Simulation and Applied Optimization, ICMSAO 2019 2019. https://doi.org/10.1109/ICMSAO.2019.8880291.

[14] Liu W, Chen Y, Wang L, Liu N, Xu H, Liu Z. An Integrated Planning Approach for Distributed Generation Interconnection in Cyber Physical Active Distribution Systems. IEEE Transactions on Smart Grid 2020;11:541–54. https://doi.org/10.1109/TSG.2019.2925254.

[15] Mahdad B. Optimal reconfiguration and reactive power planning based fractal search algorithm: A case study of the Algerian distribution electrical system. Engineering Science and Technology, an International Journal 2019;22:78–101. https://doi.org/10.1016/J.JESTCH.2018.08.013.

[16] Muminovic Z, Dedovic MM, Avdakovic S. Optimal capacitor placement in low voltage distribution grid. ICAT 2019 - 27th International Conference on Information, Communication and Automation Technologies, Proceedings 2019. https://doi.org/10.1109/ICAT47117.2019.8938988.

[17] Hao Y, Yi Y, Tang J, Shi M. Active Reactive Power Control Strategy Based on Electrochemical Energy Storage Power Station. 2019 3rd IEEE Conference on Energy Internet and Energy System Integration: Ubiquitous Energy Network Connecting Everything, EI2 2019 2019:90–4. https://doi.org/10.1109/EI247390.2019.9062188.

[18] Chen J, Xu J, Zhong S. Optimal Voltage Control for Active Distribution Networks. ISPEC 2019 - 2019 IEEE Sustainable Power and Energy Conference: Grid Modernization for Energy Revolution, Proceedings 2019:382–91. https://doi.org/10.1109/ISPEC48194.2019.8974988.

[19] Huang Z, Fang B, Deng J. Multi-objective optimization strategy for distribution network considering V2G-enabled electric vehicles in building integrated energy system. Protection and Control of Modern Power Systems 2020;5. https://doi.org/10.1186/s41601-020-0154-0.

[20] Saffari M, Kia M, Vahidinasab V, Mehran K. Integrated active/reactive power scheduling of interdependent microgrid and EV fleets based on stochastic multi-objective normalised normal constraint. IET Generation, Transmission & Distribution 2020;14:2055–64. https://doi.org/10.1049/IET-GTD.2019.1406.

[21] Alayi R, Kasaeian A, Atabi F. Optical modeling and optimization of parabolic trough concentration photovoltaic/thermal system. Environmental Progress & Sustainable Energy 2020;39:e13303. https://doi.org/10.1002/EP.13303.

[22] Marefati M, Shamel A, Alayi R, Gholaminia B, Rohi H. Designing a PID controller to control a fuel cell voltage using the imperialist competitive algorithm. Advances in Science and Technology Research Journal 2016;Vol. 10:176–81. https://doi.org/10.12913/22998624/62629.

[23] Zhang X, Liu J, Liu T, Zhou L. A novel power distribution strategy for parallel inverters in islanded mode microgrid. Conference Proceedings - IEEE Applied Power Electronics Conference and Exposition - APEC 2010:2116–20. https://doi.org/10.1109/APEC.2010.5433528.

[24] Lappalainen K, Valkealahti S. Output power variation of different PV array configurations during irradiance transitions caused by moving clouds. Applied Energy 2017;190:902–10. https://doi.org/10.1016/J.APENERGY.2017.01.013.